

Effect of cathode structure on cell performance in wireless charging process

Shao-Kang Hu^a, Tse-Chuan Chou^{a,*}, Bing-Joe Hwang^b

^a Department of Chemical Engineering, National Cheng Kung University, Tainan 701, Taiwan

^b Department of Chemical Engineering, National Taiwan University of Science and Technology, Taipei 106, Taiwan

Available online 3 June 2005

Abstract

The application of micro-systems, designed to contain monitoring or actuating devices is often hampered by energy supply. For systems with low power demands, the use of implanted battery and inductive links for wireless energy transfer to the remote system is widely acknowledged solution. But these energy supply system are limited by the energy shortage and inductive coils alignment. The misalignment of wireless energy transfer loops causes the low energy transfer efficiency and inexact induced potential. Although the implanted battery can offer more stable energy supply, the shortage in energy storage limited its application and durability. In this work, we developed the wireless microwave charging module to overcome the disadvantages of previous methods. The wireless microwave charging module can charge the implanted lithium ion battery in a suitable distance by tuning the power input and the implanted lithium ion battery shows excellent cycleability after 20 cycles of wireless charging. Although the conversion of the wireless microwave charging is only 2–5%, it can be improved by using other designs of antenna (microwave generation part) and rectify antenna (receive and conversion part). The cell performance of the spinel compound for the wireless energy transfer is better than that of the layered compound.

© 2005 Elsevier B.V. All rights reserved.

Keywords: Microwave wireless charging; Lithium ion battery; Implanted battery; Structure

1. Introduction

Wireless power transmission (WPT) has been proposed for many years and is expected to be one of the most promising energy transfer methods in the near future [1–5], especially in space power supply and emergency power recovery. However, short-range and low-power microwave WPT has not been well developed. The short-range and low-power WPT can be extensively applied in micro-systems such as implanted pace-makers, implanted medical micro-systems and sensors.

To improve the performance of a conventional wireless power transmission system, we develop an implantable energy storage system with a rechargeable lithium ion battery which can be charged by a wireless microwave charging

module. The wireless microwave charging device with a suitable capacitor has been reported for rechargeable lithium ion battery in our previous study [6]. Since rechargeable lithium ion batteries have long cycle life, high energy density and good safety record, they are good candidates for implanted power sources. Traditionally, a primary battery is used as implanted power source, since there is no efficient way to charge the power source (i.e. a rechargeable battery). A capacitor charged by a body-mounted rf-generator with two inductively coupled loop antennas is also employed for an implanted power source. Recently wireless power transmission (WPT) is considered to be a potential way to charge an implanted battery. WPT can deliver power without any circuit connection to a device. The first demonstration of WPT was successfully completed in 1976 by NASA [7–10]. WPT techniques can also be employed in remote micro-systems such as medical microsensors. The service life of a system with a rechargeable battery can be improved if WPT can be utilized effectively. To reveal the difference in conventional

* Corresponding author. Tel.: +886 6 2757575x62639;

fax: +886 6 2366836.

E-mail address: tcchou@mail.ncku.edu.tw (T.-C. Chou).

and WPT charging process, a conventional charging process is chosen as a blank test for comparison in this study. A conventional charging procedure includes two steps, in which the battery is initially charged by a constant current until the potential reaches the upper voltage limit and then by a constant voltage until the current reaches a predetermined value. Microwaves in WPT are converted directly into dc power by a receiving antenna (rectenna). A wireless charging module can charge an implanted energy storage device without any mounted device and physical contact. In order to investigate the feasibility for using a wireless charging module to charge an implanted energy storage device a rectenna array with a charging circuit embedded in a pig's skin tissue was used to simulate the implanted system. In this work, the cell performance of the implanted lithium ion batteries made of the cathodes with spinel or layered structures were investigated.

2. Experiment

2.1. Cathode material synthesis

Nano-sized $\text{LiNi}_{0.45}\text{Mn}_{0.45}\text{Co}_{0.1}\text{O}_2$ powders were synthesized by the sol-gel method using citric acid as a chelating agent [11–13]. Stoichiometric amounts of lithium acetate ($\text{Li}(\text{CH}_3\text{COO})\cdot 2\text{H}_2\text{O}$), nickel acetate ($\text{Ni}(\text{CH}_3\text{COO})_2\cdot 4\text{H}_2\text{O}$) and cobalt nitrate ($\text{Co}(\text{NO}_3)_2\cdot 6\text{H}_2\text{O}$) were dissolved in distilled water and mixed with an aqueous solution of citric acid. The resulting solution was mixed with a magnetic stirrer at 80–90 °C for 5–6 h to obtain a clear viscous gel. The gel was dried in a vacuum oven at 140 °C for 24 h. The layered $\text{LiNi}_{0.45}\text{Mn}_{0.45}\text{Co}_{0.1}\text{O}_2$ compounds were ground and calcined at 750–900 °C after precalcining the precursor at 450 °C. The heating and cooling rate of the heat treatment was 2 °C min^{-1} .

The Li, Co and Ni contents in the resulting materials were analyzed using an inductively coupled plasma/atomic emission spectrometer (ICP/AES, Kontron S-35). The phase purity was verified from powder X-ray diffraction measurements (XRD, Rigaku D/max-b) using $\text{Cu K}\alpha$ radiation. The particle morphology of the powders after calcination was obtained using a scanning electron microscopy (SEM, Hitachi S-4100). Electrochemical characterization was carried out with a coin-type cell. The synthesized $\text{LiNi}_{0.45}\text{Mn}_{0.45}\text{Co}_{0.1}\text{O}_2$ and commercial spinel LiMn_2O_4 (Merck) cathode were prepared by mixing an 85:3.5:1.5:10 (w/w) ratio of active materials, carbon black, KS6 graphite and polyvinylidene fluoride binder, respectively, in *N*-methyl pyrrolidinone. The resulting paste was cast on an aluminum current collector. The entire assembly was dried under vacuum overnight and then heated in an oven at 120 °C for 2 h. Lithium metal (FMC) was used as an anode and a polypropylene separator was used to separate the anode and the cathode. 1.0 M LiPF_6 dissolved in a 1:1 mixture of ethylene carbonate (EC)/diethyl carbonate (DEC) was used as an

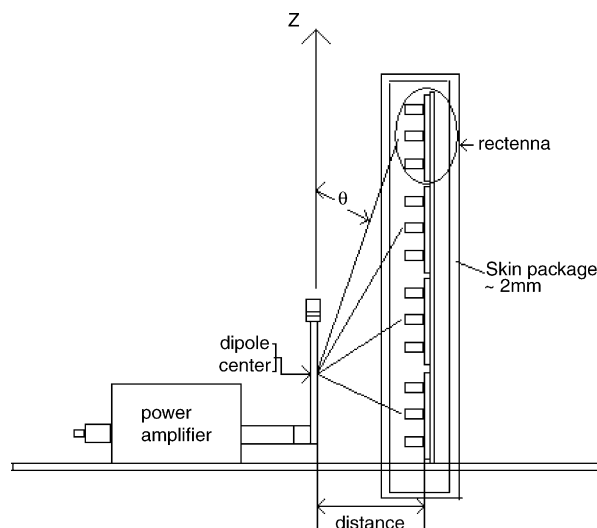


Fig. 1. Power transmitter and rectenna modules packed in a pork skin tissue.

electrolyte. The cells were assembled in an argon-filled dry box where both the moisture and oxygen contents were less than 1 ppm.

2.2. Wireless microwave charging test

The scheme of the wireless power transmission system developed in this study is shown in Fig. 1. The wireless power transmission module includes a continuous 900 MHz microwave generator and a rectenna array. The rectenna (rectify antenna) array is embedded in pig's skin tissue (ca. 2 mm in thickness) to simulate a wireless power transmission system implanted in a human body. This power transmit module can transmit microwave power to air and receiver steadily. The rf/dc conversion component is able to convert the transmitted power and charge a lithium ion battery. The capacitor in the charging circuit is set in parallel with the fabricated lithium ion battery to modify the converted dc power [6]. The charging cycles are carried out over a potential range of 3.0–4.3 V.

3. Results and discussion

The converted potential profile of the packed rectenna array is shown in Fig. 2. The open circuit potential and conversion efficiency depend on the conditions such as the distance between the antenna and the rectenna array (receiver), the ambient media of the rectenna array, the efficiency of the rectenna array and the energy consumption of the charging circuit. The output of the antenna (generator) was set at 40 mW. It was found that the converted potential is disproportional to the distance between the antenna and the rectenna array. The rectified open circuit potential obtained from the charging circuit with a capacitor in parallel decreases from 4.64 to 0.565 V with an increase

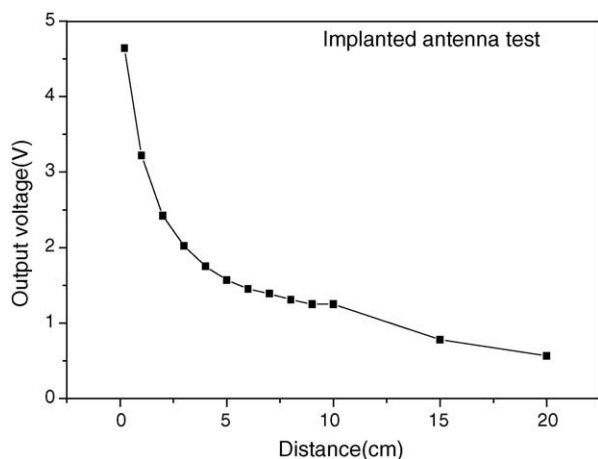


Fig. 2. Converted potential vs. distance between antenna and implanted rectenna array for 900 MHz wireless microwave charging module.

in the distance from 0.2 to 20 cm, respectively, in the studied setup. The conversion efficiency of this wireless charging module is found to be only about 2–5% in the studied setup, indicating that it can be further improved by focusing the microwave radiation and minimizing the energy consumption of the conversion circuit in the future. Meanwhile, the dependence of the cell performance in the wireless charging process on the cathode structure is also of great interest. The synthesized $\text{LiNi}_{0.45}\text{Mn}_{0.45}\text{Co}_{0.1}\text{O}_2$ material with layered structure and the commercial LiMn_2O_4 material with spinel structure were chosen to study the dependence.

To simulate an implanted wireless charging process the rectenna array was packed in a pig's skin tissue (ca. 2 mm in thickness). The cycleability for the $\text{LiNi}_{0.45}\text{Mn}_{0.45}\text{Co}_{0.1}\text{O}_2$ cathode charged by the conventional charging process at 0.1 C rate and the wireless charging process is shown in Fig. 3. The initial discharge capacity (162 mAh g^{-1}) of the $\text{LiNi}_{0.45}\text{Mn}_{0.45}\text{Co}_{0.1}\text{O}_2$ cathode is pretty high in the

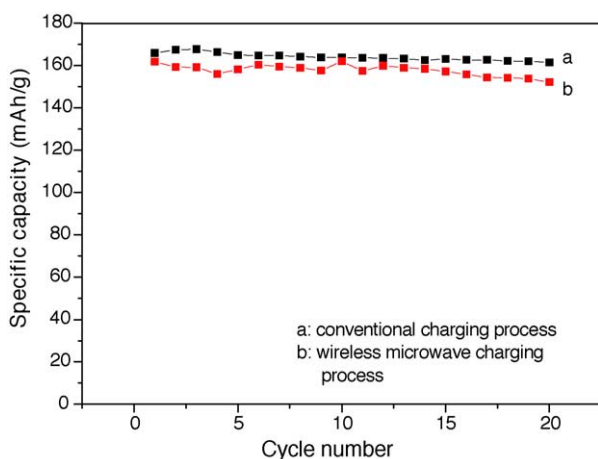


Fig. 3. Charge/discharge capacity vs. cycle number of the synthesized $\text{LiNi}_{0.45}\text{Mn}_{0.45}\text{Co}_{0.1}\text{O}_2$ in a range of 3.0–4.3 V: (a) conventional charging process and (b) wireless microwave charging process.

wireless charging process and similar to that (168 mAh g^{-1}) obtained in the conventional process in the potential range of 3.0–4.3 V. The discharge capacity of the synthesized $\text{LiNi}_{0.45}\text{Mn}_{0.45}\text{Co}_{0.1}\text{O}_2$ cathode is higher than that of the $\text{LiCo}_x\text{Ni}_{1-x}\text{O}_2$ cathode at same charging-discharging conditions [14–16]. The higher discharge capacity results from the changes of the redox pair reaction from $\text{Ni}^{3+}/\text{Ni}^{4+}$ in $\text{LiCo}_x\text{Ni}_{1-x}\text{O}_2$ to $\text{Ni}^{2+}/\text{Ni}^{4+}$ in $\text{LiNi}_{0.45}\text{Mn}_{0.45}\text{Co}_{0.1}\text{O}_2$. Meanwhile, the presence of manganese in $\text{LiNi}_{0.45}\text{Mn}_{0.45}\text{Co}_{0.1}\text{O}_2$ leads to an oxide network more favorable for lithium ion intercalation. It was also found that the capacity retention in the conventional charging process is better than that in the wireless charging process. The reason for the serious capacity fading in the wireless microwave process is due to the poor quality of the converted dc power. The ripple of the converted dc power in the wireless charging process is more serious than that in previous work and the rapid potential vibration may directly affect the capacity retention of the cell [6]. In order to investigate the relationship of the structure and the capacity fading, X-ray powder diffraction was used to examine the structural changes of these cathode materials charged in different ways.

Shown in Fig. 4 are the XRD patterns for the fabricated $\text{LiNi}_{0.45}\text{Mn}_{0.45}\text{Co}_{0.1}\text{O}_2$ batteries charged by the wireless charging process and the conventional charging process. All the peaks appearing on the XRD pattern were identified with the characteristics peaks of $\text{LiNi}_{1-x-y}\text{Co}_x\text{Mn}_y\text{O}_2$ reported in the X-ray powder data file of JCPDS. No impurity related peaks have been observed from the XRD pattern of these samples. It reveals that all the charged samples exhibit some structural changes. It is particularly interesting to note that the value of I_{003}/I_{104} for the $\text{LiNi}_{0.45}\text{Mn}_{0.45}\text{Co}_{0.1}\text{O}_2$ material charged by different processes. The intensity ratio is reported to be closely related to the undesirable cation mixing which is reduced as the value of the ratio is increased [17–19]. The value of I_{003}/I_{104} for the hexagonal unit

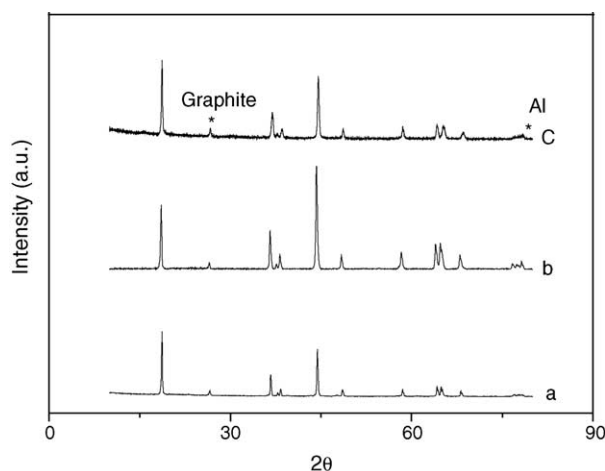


Fig. 4. XRD patterns for the layer $\text{LiNi}_{0.45}\text{Mn}_{0.45}\text{Co}_{0.1}\text{O}_2$: (a) pristine, (b) charged by a wireless microwave charging process and (c) charged by a conventional process.

Table 1
 I_{003}/I_{104} ratio of different treated samples

	I_{003}	I_{104}	I_{003}/I_{104}
Pristine	14.4	10.61	1.36
Charged by a wireless microwave charging process	9.96	16.09	0.54
Charged by a conventional charging process	6.30	5.065	1.244

cell of these samples charged by different processes was determined and shown in Table 1. It indicates the cation mixing is more serious in the wireless charging process than that in the conventional charging process.

In order to overcome the serious capacity fading of the layered cathode material in the wireless microwave process, the commercial spinel LiMn_2O_4 was selected to be instead of the layered one. The fabricated spinel battery was also charged in conventional charging process and wireless microwave charging process in the potential range of 3.0–4.2 V. The cycleability of the spinel LiMn_2O_4 battery charged by the conventional charging process at 0.1 C rate and the wireless charging process are given in Fig. 5. It can be seen that the cell performance of the spinel LiMn_2O_4 charged by the wireless charging process is as good as that by the conventional process. The capacity fading for the spinel cathode in the wireless charging process and the conventional charging process is 2.7 and 1.9%, respectively. In order to discover the structural change of these samples, the XRD patterns of the charged and pristine samples are shown in Fig. 6. All the peaks appearing on the XRD pattern were identified with the characteristics peaks of LiMn_2O_4 reported in the X-ray powder data file of JCPDS. It reveals that all the charged samples exhibit no structural changes and no impurity related peaks has been observed from the XRD pattern of these samples. These observations demonstrate the ripple potential in the converted dc power does not affect the cell performance of the battery with a spinel cathode. This result may due to the high

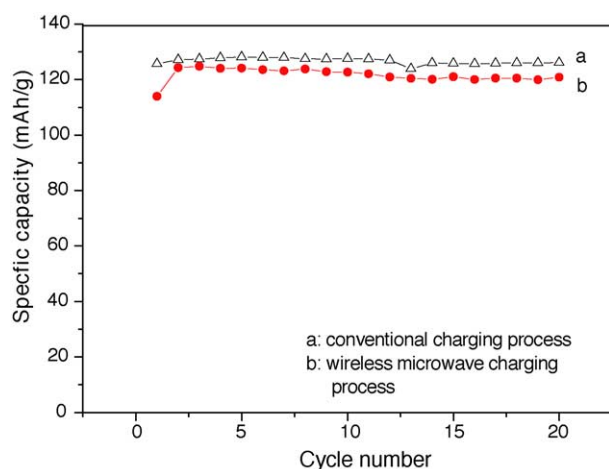


Fig. 5. Charge/discharge capacity vs. cycle number of commercial LiMn_2O_4 in a range of 3.0–4.2 V: (a) conventional charging process and (b) wireless microwave charging process.

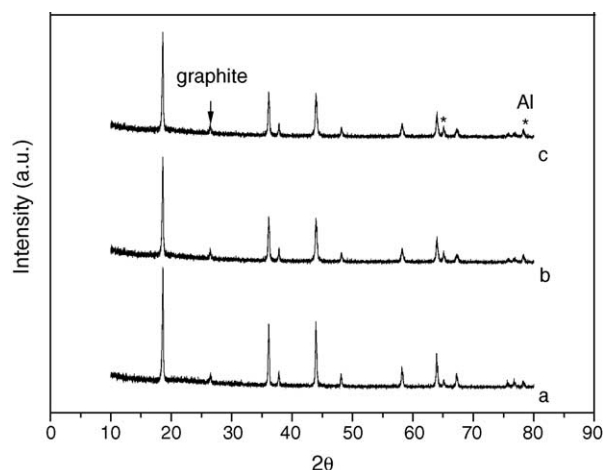


Fig. 6. XRD patterns for commercial LiMn_2O_4 : (a) pristine, (b) charged by a wireless microwave charging process and (c) charged by a conventional process.

structural stability and equal lattice expansion and shrinkage in spinel LiMn_2O_4 during the discharging and charging processes [20–22].

Comparing the capacity fading between the layered $\text{LiNi}_{0.45}\text{Mn}_{0.45}\text{Co}_{0.1}\text{O}_2$ cathode and the spinel LiMn_2O_4 cathode charged by a wireless charging process, the spinel LiMn_2O_4 cathode shows lower capacity fading and better structural stability. From these results, it can be concluded that the spinel structure cathode material is more suitable to be applied in a wireless microwave charging process.

4. Conclusions

The effect of cathode structure on the cell performance in the wireless charging process with an implanted rectenna array was investigated. The spinel LiMn_2O_4 cathode shows better capacity retention and structure stability than the layered $\text{LiNi}_{0.45}\text{Mn}_{0.45}\text{Co}_{0.1}\text{O}_2$ cathode in the wireless charging process. It can be also concluded that the lithium ion battery made of cathode with spinel structure is more suitable to be applied in a wireless microwave charging process and can offer the micro-system a steady energy supply.

Acknowledgements

Financial support from the Ministry of Education (Ex: 91-EX-FA09-5-4), Taiwan, and from NCKU and NTUST, Taiwan, Republic of China are gratefully acknowledged.

References

- [1] K. O'Brien, G. Scheible, H. Gueldner, IEEE 34th Annu. Conf. Power Electronics Specialist 4 (2003) 15–19.
- [2] N. Mitumoto, K. Tsuruta, T. Shibata, N. Kawahara, Int. Symp. Micro-mechatronics Human Sci. (2001) 57–62.

- [3] Y.H. Park, D.G. Youn, K.H. Kim, Y.C. Rhee, TENCON 99, Proc. IEEE Region 10 Conf. 2 (1999) 1423–1426.
- [4] V.M. Shokalo, D.V. Gretsikh, A.M. Rybalko, IVth Int. Conf. Antenna Theory Techniques 2 (2003) 846–851.
- [5] Y.H. Suh, K. Chang, Microwave Theory Techniques 50 (2002) 1784–1789.
- [6] S.K. Hu, T.C. Chou, B.J. Hwang, Transactions on Industrial Electronics, submitted for publication.
- [7] D.G. Youn, Y.H. Park, K.H. Kim, Y.C. Rhee, TENCON 99, Proc. IEEE Region 10 Conf. 2 (1999) 1419–1422.
- [8] J.C. Lin, Microwave Mag. 3 (2002) 36–42.
- [9] J.O. McSpadden, J.C. Mankins, Microwave Mag. 3 (2002) 46–57.
- [10] G. Scheible, J. Schutz, C. Apneseth, IEEE 2002 28th Annu. Conf. Ind. Electronics Soc. 2 (2002) 1358–1363.
- [11] B.J. Hwang, R. Santhanam, D.G. Liu, Y.W. Tsai, J. Power Sources 102 (2001) 326–331.
- [12] B.J. Hwang, R. Santhanam, D.G. Liu, J. Power Sources 101 (2001) 86–89.
- [13] B.J. Hwang, R. Santhanam, S.G. Hu, J. Power Sources 108 (2002) 250–255.
- [14] Y. Sun, C. Ouyang, Z. Wang, X. Huang, J. Electrochem. Soc. 151 (2004) 504–A508.
- [15] K.B.R. Gover, R. Kanno, B.J. Mitchell, M. Yonemura, Y. Kawamoto, J. Electrochem. Soc. 147 (2000) 4045–4051.
- [16] B.J. Hwang, Y.W. Tsai, D. Carlier, G. Ceder, Chem. Mater. 15 (2003) 3676–3682.
- [17] J. Kim, K. Amine, J. Power Sources 104 (2002) 33–39.
- [18] Y. Gao, M.V. Yakovleva, W.B. Ebner, Electrochem. Solid-State Lett. 1 (1998) 117–119.
- [19] J. Cho, G. Kim, H.S. Lim, J. Electrochem. Soc. 146 (1999) 3571–3576.
- [20] B.J. Hwang, R. Santhanam, D.G. Liu, Y.W. Tsai, J. Power Sources 102 (2001) 326–331.
- [21] G. Amatucci, J.M. Tarascon, J. Electrochem. Soc. 149 (2002) K31–K46.
- [22] B.J. Hwang, Y.W. Tsai, R. Santhanam, Y.W. Wu, S.G. Hu, J.F. Lee, D.G. Liu, J. Power Sources (2003) 206–215.